Polymer Testing 112 (2022) 107642

Contents lists available at ScienceDirect

Polymer Testing

journal homepage: www.elsevier.com/locate/polytest

Polyethylene/ poly(3-hydroxybutyrate-co-3-hydroxyvalerate /carbon nanotube composites for eco-friendly electronic applications

David Fernández Armada [a], Victoria González Rodríguez [a], Pedro Costa [b], Senentxu Lanceros-Mendez [b,c,d], Goretti Arias-Ferreiro [a], María-José Abad [a], Ana Ares-Pernas [a,*]

[a] Universidade da Coruña, Campus Industrial de Ferrol, Grupo de Polímeros, Centro de Investigacións Tecnolóxicas, 15403, Ferrol, Spain
[b] Center/Department of Physics, Minho University, 4710-058, Braga, Portugal
[c] BCMaterials, Basque Center for Materials, Applications and Nanostructures, 48940, Leioa, Spain
[d] Ikerbasque, Basque Foundation for Science, 48009, Bilbao, Spain

ARTICLE INFO

Keywords:
PHBV
Polymer composites
Carbon nanotubes
Electrical conductivity
Rheology
EMI

ABSTRACT

The development of new conducting composites, for electric and electronic applications, with lower environmental impact is a relevant issue. Blending poly (3-hydroxybutyrate-co-3-hydroxyvalerate (PHBV) with high-density polyethylene (HDPE), 50/50 HDPE/PHBV, and multiwalled carbon nanotubes (MWCNTs) (3.5 and 7.5%), represents a suitable strategy for improving sustainability of conducting polymers while maintaining procesability and functional performance. The study focuses on thermal, mechanical, morphological, rheological, electrical properties and EMI shielding effectiveness. Composites show a morphology in which MWCNTs remains in HDPE phase. Without compatibilizer, only the composite with 7.5% of MWCNTs achieves a conductivity value suitable for reaching 20 dB of electromagnetic shielding. In composites with PE grafted with maleic anhydride (0.5%) the electrical conductivity substantially increased, achieving a suitable EMI shielding level with lower proportion of nanotubes (5 wt%). Summarizing, composites with reduced environmental impact, suitable for EMI shielding applications, have been obtained optimizing the MWCNTs amount and their dispersion.

1. Introduction

The dispersion of conductive fillers such as carbon nanofibers [1,2], carbon nanotubes [3–7], graphene [8,9], carbon black [10,11] and others, in a polymer matrix can result in electrical conductive polymer composites (CPCs) that are frequently used to manufacture products with electrical properties for designing sensors, electronic devices and for EMI shielding applications. In the latter, CPCs are needed that combine ease of processability and molding, low cost, light weight and resistance to environmental conditions in addition to high level of shielding. Amongst different possible fillers, single-walled or multi-walled carbon nanotubes (MWCNTs) show exceptional electrical properties and high aspect ratio and they are frequently used in electrical and EMI shielding applications [12–18].

CPCs can be obtained by means of filler dispersion in a polymer matrix or in a blend. The use of an immiscible polymer blend as matrix can lead to preferential localization of nanofiller in one or other phase (or even at the interface between the two polymers), resulting in a segregated conductive network which has demonstrated to be effective for achieving high electrical properties (conductivity, EMI shielding) using a low amount of filler [19–26]. For example, Wang et al. studied in a review like various multiple structures improve EMI shielding behaviour [27]. A control distribution of MWCNTs in isotactic polypropylene/poly (ethylene-co-1-octene) blends is used too by Liu et al. to construct high-efficiently conductive networks resulting in a low percolation threshold, high performance electrical conductivity and electromagnetic interference shielding [28] effectiveness. Other example is the study performed by Tian-Ning in which tunable electrical conductivity and microwave shielding performance were obtained by controlling the distribution of MWCNTs in polyethylene/poly (ethylene-co-1-octene) [29] blends.

On the other hand, environmental problem caused by plastic waste is leading the development of environmentally sustainable materials that can replace current plastics. For this reason, application of biopolymers is increasing in all fields of sciences and technology [30,31]. For example, Ebrahimi et al. incorporated titanium dioxide in a poly (L-lactide)-b-poly (ε-capolactone) improving thermal and mechanical properties [32,33]. Poly (3-hydroxybutyrate-co-3-hydroxyvalerate)

* Corresponding author.
E-mail address: ana.ares@udc.es (A. Ares-Pernas).

https://doi.org/10.1016/j.polymertesting.2022.107642
Received 20 January 2022; Received in revised form 26 April 2022; Accepted 15 May 2022
Available online 17 May 2022

(PHBV), a bio-based, biodegradable and biocompatible polymer produced naturally by bacteria, is being used as alternative for many non-biodegradable synthetic polymers. Blending PHBV with conventional polymers represents a good strategy for developing more sustainable composites and extend the properties range of pristine polymers [30,31,34]. HDPE/PHBV blends with different compositions have been reported with good mechanical, chemical and thermal properties or even with improved barrier properties for packaging applications [35–37]. Although the combination of bio-based and biodegradable polymers with synthetic polymers may have influence on the biodegradation of polymeric material [38] the obtained blend continues being biodegradable. Besides, the addition of conductive fillers in PHBV matrix not compromise its biodegradability, although the biodegradation rate decreases [39–41].

Heterogeneous polymer blends formed with PHBV and a conventional polymer (as polyethylene), with a segregated conductive network (which allows an appropriate distribution of filler inside), could obtain good electrical properties with low filler amounts while decreasing environmental impact of similar composites. On the whole, the addition of MWCNT in HDPE/PHBV blends with a suitable morphology, constituted a promising approach towards more sustainable conductive polymer composites. The literature presents some few works related with biopolymer and synthetic polymer blends loaded with MWCNT [42,43]. As an example Tan et al. studied the effect of phase morphology and distribution of MWCNTs in poly (ε-caprolactone)/poly (L-lactide) blends on microwave shielding obtaining promising results with a sea-island morphology [44] and even best with a sandwich structure. Nevertheless, to the best of our knowledge, this work is the first study on feasibility of HDPE/PHBV blends filled with MWCNTs to obtain conductive polymer composites for EMI shielding applications.

In spite of the intrinsic conductivity of MWCNTs and their high aspect ratio, low percolation threshold in polymer matrices prepared by blend melting is not easily achieved due to the tendency of MWCNT to agglomerate because attractive van der Waals forces. To overcome this drawback, it is important to select the appropriate processing conditions, but also, to perform a surface treatment of the MWCNTs which optimizes their dispersion into the polymer matrix and/or to use an appropriate compatibilizer, to improve the interfacial adhesion between polymer and fillers. As a result, other properties like mechanical strength and electrical conductivity are also improved. The employment of maleic anhydride grafting polymers is a common strategy to compatibilize polymeric blends. In addition, ionic liquids has proven to be successful in PP/PLA blends filled with MWCNT improving considerably electrical conductivity and electromagnetic interference shielding effectiveness [43]. However, the use of ionic liquids is more expensive and their use on an industrial scale is more complex.

The main goal in this work is the development of new conducting polymer composites based on 50/50 HDPE/PHBV matrix using MWCNT as conductive filler. To achieve improved electrical performance, the composites were designed to obtain a segregated conductive network, which maximises the properties with lower filler amounts. In order to improve the dispersion of the MWCNTs, an ethylene and anhydride maleic copolymer was used as compatibilizer. The study was focused on thermal, mechanical and electrical properties of composites, as well as on the effectiveness of the new composites in EMI shielding applications.

The data show that the use of polyethylene grafted with maleic, at low amounts, improves the electrical properties and consequently the EMI shielding performance obtained by nanocomposites. These results are related to morphological changes by improving the dispersion of CNTs in the matrix and better adhesion between the PHBV and PE phases.

2. Experimental

2.1. Materials

A poly (3-hydroxybutyrate-co-3-hydroxyvalerate) (PHBV Nature-Plast PHI 002 supplied by Natureplast) (density: 1.23 g/cm^3 and Melt flow rate:5–10 g/min (190 °C, 2.16 kg)) and a high density polyethylene (HDPE 25055E supplied by Down Chemical Iberica, S.L.) (density: 0.955 g/cm^3 and Melt flow index:25 g/min (190 °C, 2.16 kg)) were used as polymeric matrix. The nanotubes were incorporated into the polymeric matrix from a masterbatch based on high density polyethylene loaded with 15 wt% of MWCNT (Plasticyl HDPE1501 supplied by Nanocyl S.A, Sambrevile, Belgium). MWCNTs (characterized according to the supplier) present an average diameter of 9.5 nm, a length of 1.5 μm, a carbon purity of 90% and a surface area of 250–300 m^2 g^{-1}. A random ethylene copolymer, incorporating a 12% of monomer, which is classified as being a maleic anhydride (MAPE) (FUSABOND M603 by Down Chemical) was used as a compatibilizer. It shows a density of 0.94 g/cm^3 and a Melt Flow Rate of 25 g/10 min (190 °C, 2.16 kg).

2.2. Preparation of the composites

Table 1 shows the composite formulations with 50/50 HDPE/PHBV ratio and different contents of MWCNT. The MWCNT masterbatch was diluted with the same HDPE. The 50/50 proportion of HDPE/PHBV was selected in order to obtain a more sustainable and affordable material for the industry. On the other hand, in this proportion, HDPE/PHBV blend is immiscible, which will help to obtain a segregated conducting network in the composite.

Before extrusion, PHBV was dried in an oven at 80 °C for 4 h. Then, the different composites were extruded using a miniextruder equipped with twin conical co-rotating screws and a capacity of 7 cm^3 (Minilab HaakeRheomex CTW5, Thermo Scientific). The extrusion was carried out in two steps: in the first step, the masterbach was diluted with HDPE, in order to obtain the desired amount of MWCNTs, using a rotation rate of 40 rpm, a temperature of 190 °C and a residence time of 3 min; during a second extrusion step (at 190 °C and 40 rpm for 3 min), PHBV was incorporated into the HDPE/MWCNT blend. The maleic anhydride grafted polyethylene used as compatibilizer, was added in the second step of extrusion. Composite formulations and their nomenclature are displayed in Table 1.

The samples for the different tests were injection moulded in circular specimens (diameter of 25 mm and thicknesses of 1.5 mm) and prismatic specimens (2 × 4x10 mm) using a Haake MiniJet Pro injection molding machine (Thermos Scientific) at 190 °C, applying 800 bar for 10 s.

Table 1
Raw materials, binary blends and composites formulation. Rheological cross-over points of different formulations.

Sample	PE (wt. %)	PHBV (wt.%)	MWCNT (wt.%)	Compatibilizer (wt.%)	ωc; Gc (rad.s^{-1}; Pa)
HDPE	100	-	-	-	G''>G′
PHBV	-	100	-	-	G''>G′
HDPE/ PHBV	50	50	-	-	G''>G′
M1	46.25	46.25	7.5	-	G'>G″
M2	47.50	47.50	5	-	G'>G″
M3	48.50	48.50	3	-	1.53; 4583
M1*	46.00	46.00	7.5	0.5	G'>G″
M2*	47.25	47.25	5	0.5	G'>G″

2.3. Sample characterization

The morphology of the composites was evaluated by Scanning Electron Microscopy (SEM). Specimens were broken under cryogenic conditions and then examined using a JEOL JSM-7200F Field Emission Scanning Electron Microscope at an accelerating voltage of 10 kV. Prior to observation, the samples were sputter-coated with a thin palladium/platinum layer (Cressintong 208HR).

The rheological measurements were performed using a controlled strain rheometer (ARES, TA Instruments) with parallel-plate geometry (25 mm diameter, 1 mm gap) at 190 °C. The complex viscosity (η*), storage modulus (G′), and loss modulus (G″) were measured as a function of frequency (ω). The rheological tests were performed in the linear viscoelastic region (LVE). This linear viscoelastic region was determined previously from a strain sweep test. The frequency sweep measurements were set up in the frequency range 1×10^{-1} to 10^{2} rad s^{-1}.

Thermal measurements were carried out with a differential scanning calorimeter (DSC 2020, TA Instruments)) under nitrogen atmosphere. The samples (6–10 mg) were heated from 0 °C to 230 °C at a rate of 10 °C.min^{-1} and mantained 5 min At 230 °C to erase their thermal history. Finally, they were cooled to 0 °C at a rate of 10 °C.min^{-1}.

The degree if crystallinity (Xc) of HDPE and PHBV were calculated by the following equation:

$$X_C = \frac{\Delta H_m}{\Delta H_{100\%}} x100 \quad (1)$$

where $\Delta H_{100\%}$ is taken to be 293.6J/g for the heat of fusion of 100% crystalline HDPE [45] and 146.6 J/g for the heat of fusion of 100% crystalline PHBV [41].

Thermogravimetric Analyses (TGA) were performed using a TGA 4000- PerkinElmer, set-up under nitrogen atmosphere supplied at a constant flow rate of 50 ml min^{-1}. The composites were subjected to a heating rate of 10.0 ± 0.1 °C.min^{-1} in the temperature range between 50 up to 700 °C.

Uniaxial tensile test were performed in an Instron dynamometer 5566 at 2 mm/min in accordance with ISO 527 standard recommendations. Stress-strain curves were obtained from these tests. Young's modulus, tensile strength and elongation at yield and at break point were determined from these curves. A minimum of six specimens were tested for each system. The average values of the mechanical parameters and their deviations were calculated.

Shore D hardness values were also determined by using a Durotech MD-202 durometer in accordance with ISO 868 standard. The measurements were carried out 15 s after the durometer tip had touched the sample. All mechanical tests were performed at room temperature and at least six measurements were performed for each sample.

The electrical conductivity (σ) at room temperature was calculated from the electrical resistance data by the four-probe method (LORESTA-GP, Mitsubishi Chemical, MCP-T610). The electrical conductivities reported for each formulation are the mean values of at least 12 readings determined on three different samples.

Dielectric measurements were carried out at room temperature with a Quadtech 1920 Precision LCR Meter in the 20 Hz-1 MHz frequency range with an applied voltage of 1 V. Five millimeter diameter gold electrodes were sputtered with a ~25 nm thin gold layer, using a Polaron SC502 sputter coater under nitrogen atmosphere. The capacity (C) and dielectric losses (tan δ) were obtained as a function of frequency (ν). The real and imaginary part of the dielectric constant (ε′and ε'') and real part of the conductivity function (σ′) were obtained according to:

$$\varepsilon' = \frac{C.d}{\varepsilon_0.A'} \quad (2)$$

$$tan\delta = \frac{\varepsilon''}{\varepsilon'} \quad (3)$$

$$\sigma' = \varepsilon_0 \omega \varepsilon'' \quad (4)$$

where A indicates the plate area, d is the plate distance (samples thickness), ε_0 (8.85×10^{-12} F m^{-1}) is the permittivity of free space, ε′ and ε'' are the real and imaginary dielectric constants, respectively, and $\omega = 2\pi f$ is the angular frequency. With dielectric measurements data of the different composites, the classic electromagnetic theory was used to predict the shielding effectiveness (SE) data.

According to Colaneri and Shacklette for the far-field shielding, with the classic the EMI shielding is given according to equation (5):

$$SE = 10log\left(\frac{\sigma'}{32\pi f \varepsilon_0}\right) + 20\frac{d}{\delta} \quad (5)$$

where σ' (S/cm) is the bulk conductivity of the conductor, f (Hz) is the frequency, ε_0 (8.85×10^{-14} F cm^{-1}), d (cm) is sample thickness, $\mu_0 = 4.\pi.10^{-9}$ (H cm^{-1}) and $\delta = \sqrt{1/\mu_0 \pi f \sigma}$ cm, which is called "skin depth" of conductor. The skin depth is a measure of the depth to which the radiation will penetrate within the material (with a decrease in intensity of 1/e of its original strength).

The first term of Eq. (5) is the contribution to the shielding due to the single reflections to the incident wave by the front and back surfaces of the sample. The second term represents the attenuation by absorption as the wave passes though the sheet. The contribution of the multiple reflections is ignored in this model.

This model was successfully applied previously to measure the EMI shielding effectiveness of blends of PVC/polyaniline [46] and carbon nanofiber/liquid crystalline polymer composites [47] or even carbon nanotube/polycarbonate composites [19].

3. Results and discussion

3.1. Morphology characterization

The micrographs obtained by scanning electronic microscopy (SEM) for polymeric blend and composites with different amounts of MWCNTs are shown in Fig. 1a. SEM analysis were conducted to explore the location and distribution of the MWCNT within the HDPE/PHBV blend. From Fig. 1a two major observations can be drawn. The first one is the heterogeneous morphology in the case of the 50/50 HDPE/PHBV (usual in an immiscible blend) that seems a sea-island structure. The second observation is the selective location of MWCNTs in PE phase. The morphology of the phases depends on the blend composition, viscosity ratio between the components, and processing parameters (extrusion parameters in this work). The location of MWCNTs in PE phase is related with a viscosity ratio lower than 0.5 ($\eta_{PHBV}/\eta_{PE} = 0.46$, measured at 190 °C and 100 s^{-1}). HDPE/MWCNT masterbatch has a higher viscosity than PHBV. This fact makes difficult for MWCNTs that are included in HDPE masterbatch to leave HDPE and go into PHBV. As the mixture moves forward in the extruder PE melts, the continuous phase is formed but the larger part of the MWCNT do have no time to move to the other phase. Finally, it can be observed an acceptable dispersion level of nanotubes in the polyethylene matrix, as MWCNT content increases. This can be corroborated in Fig. 1b where composite M3 is shown with higher magnification.

The lack of adhesion between the HDPE and PHBV phases, due to the immiscibility between both polymers, becomes more pronounced when larger amounts of nanotubes are incorporated. It is important to note that as the percentage of nanotubes increases (from M3 with a 3% of MWCNTs to M1 with a 7.5% of MWCNTs) the surface becomes rougher and the lack of compatibility between HDPE and PHBV phases is more evident. This fact is probably related to a greater stiffness of the matrix as the amount of filler increases and therefore to a more brittle breakage of the samples.

Fig. 2 shows the effect of adding maleic anhydride grafted PE in

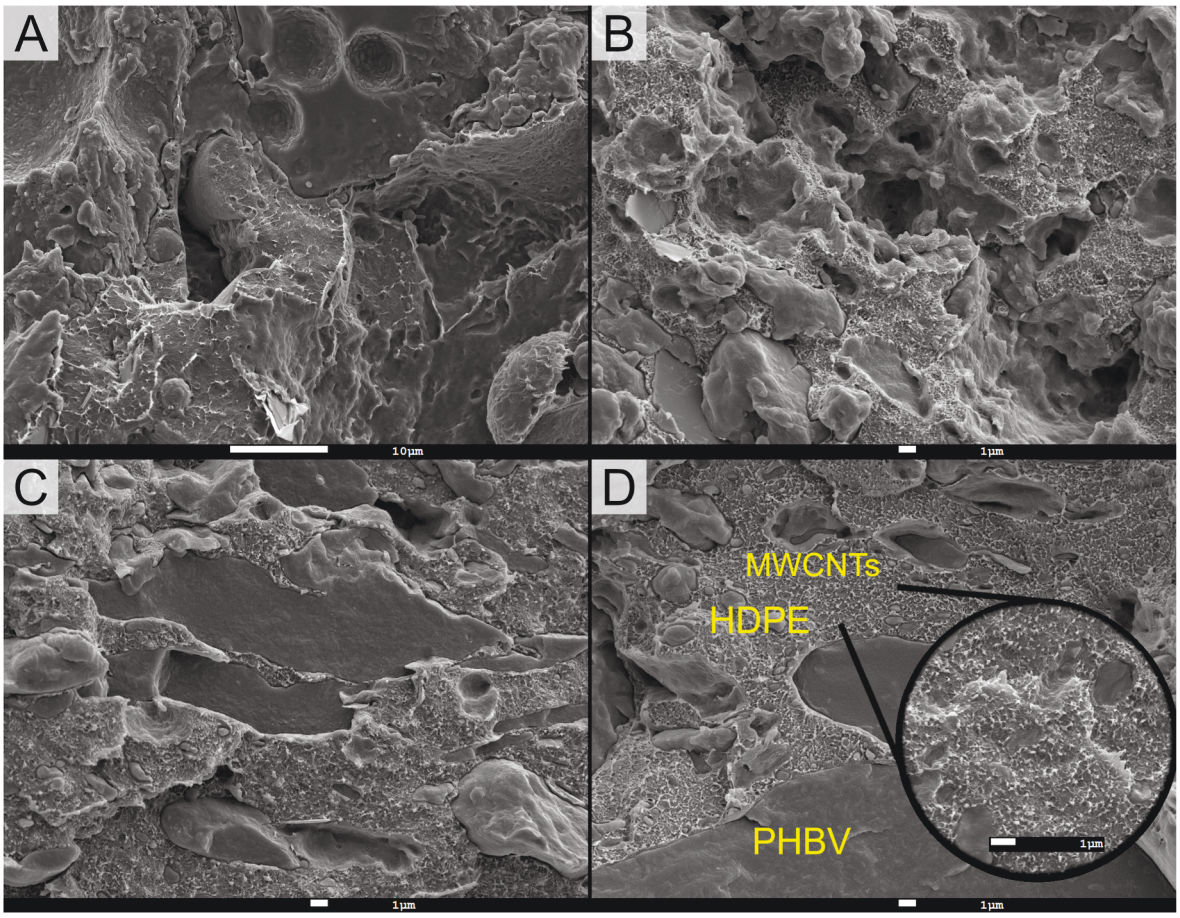

Fig. 1. SEM micrographs of A) PE/PHBV blend with magnitude amplification 2000 × , B) M1 composite, C) M2 composite and D) M3 composite, with magnitude amplification 3500 × and inset 5000 × .

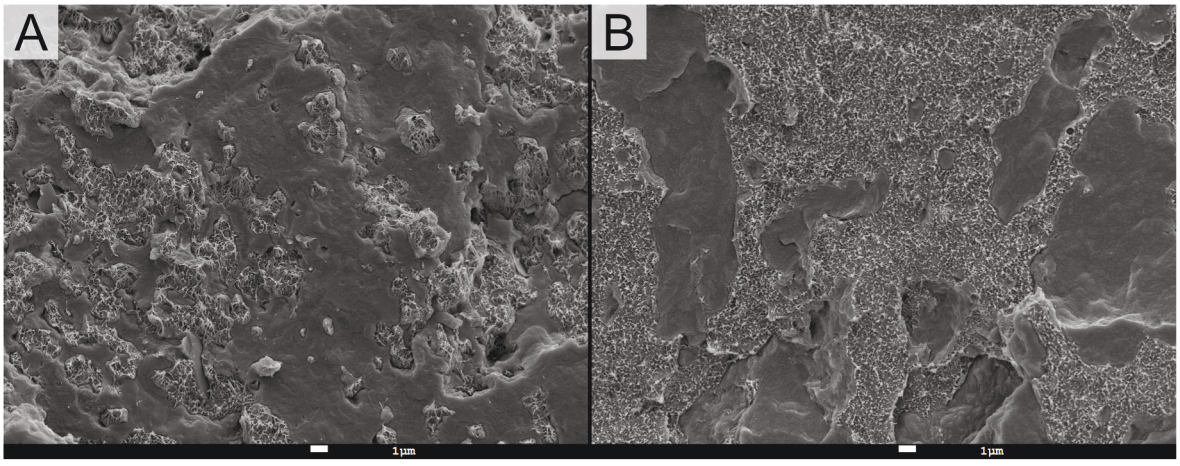

Fig. 2. SEM micrographs of PHBV/grafted-PE/MWCNT composites A) M1* and B) M2* with magnitude amplification 3500 × .

composites' morphology. The most significant consequences are that the fracture surface appears much smoother and the fracture was progressively more cohesive. The two phases appear more strongly connected and this indicates an increase in the interfacial adhesion as a result of the compatibilization effect of the maleic anhydride.

3.2. Rheological characterization

Melt rheological characterization provides information about the structure of blends and composites. Fig. 3a shows complex viscosity versus frequency. Raw polymers (HDPE and PHBV) shown a Newtonian behaviour almost in all the frequency range. Binary blend show shear-thinning behaviour, the reason for this is related to the immiscibility of both phases that prevents stress transfer between them and results in interfacial slippage. Composites shown shear thinning behaviour too as previously observed in other filled blends [48–55]. An increase in viscosity is observed with an increase in filler concentration, this increment being larger in the region of low frequencies. At high frequencies, the

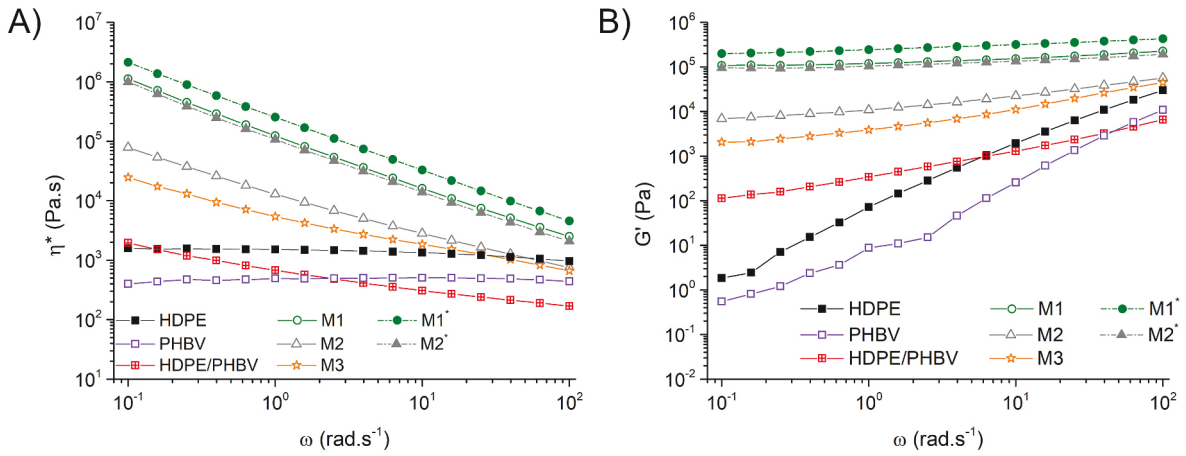

Fig. 3. Rheological parameters versus frequency; a) Complex viscosity (η*); b) Storage modulus for polymers, binary blends, and composites.

polymer chains do have not enough time to recover the original filler particle distribution. In addition, the probability of direct interaction between the filler particles rises as the concentration of filler increases making shear-thinning more noticeable.

Fig. 3b shows the frequency dependence of elastic modulus for pure polymers, unfilled HDPE/PHBV blends and composites. The effect of adding MWCNTs on the storage modulus is an increase in its value due to the interconnected network structure within the matrix, as can be observed in filled blends [48–55].

At low frequencies the fully relaxed HDPE and PHBV chains exhibit the typical Newtonian viscosity plateau with the scaling properties of approximately $G' \alpha \omega^2$, whereas the incorporation of carbon nanotubes in the polymer gradually transforms the liquid-like terminal behaviour to solid-like non terminal behaviour characterized by having G′ independent of ω. This non-terminal low frequency behaviour has been attributed to the fact that, though the polymer chain interaction still exists, the introduced nanotube-nanotube and MWCNT-polymer interactions come to dominate, eventually leading to percolation and the formation of an interconnected structure of MWCNTs in the matrix.

The crossover point (ω_c, G_c), the point at which curves of G′ and G″ against frequency intersect are also recorded in Table 1. This point is characteristic of the transition from viscous to elastic behaviour [54–56]. For pure polymers and binary blend G″ is higher than G' in all frequency range, indicating a liquid-like behaviour. For composites with low percentages of filler (3 and 5%) the behaviour does not change indicating a lack of percolation, while composite with a 7.5% of MWCNTs is percolated showing a crossover point at intermediate frequencies.

The compatibility of immiscible blends was investigated from the variation of rheological properties by adding a compatibilizer and compared with the properties previously obtained. Fig. 3a shows that, with the addition of maleic anhydride, higher values of viscosity than the immiscible blends are observed, which reflects the fact that extent of the compatibilization is increasing. This is due to the improvements of interfacial adhesion between PE and PHBV, as can be seen in the morphology (Fig. 2) and the probably better MWCNTs dispersion due to the compatibilization. In the same way higher G' values are observed in Fig. 3b.

3.3. Thermal properties

Table 2 show thermal properties obtained from DSC thermograms of the samples with similar thermal history (Fig. 4). It is shown that, the pristine polymers melt in different temperature ranges, showing well-defined melting peaks centred at 130 °C (HDPE) and 175 °C (PHBV), respectively. Regarding to crystallization temperatures (T_c), they have a value around 100 °C for HDPE and 115 °C for PHBV. 50/50 HDPE/PHBV blend shows two separate melting peaks but centred at slightly lower temperatures than the pristine thermoplastics. Besides, there is a shoulder, around 170 °C, ascribed to the heterogeneous crystallization of PHBV in the presence of HDPE. This fact is related with a lack of thermodynamic miscibility between HDPE and PHBV, as can be observed previously in rheological and morphological results and it is a typical behaviour in immiscible blends. When the MWCNTs are added, the effect in the thermal properties is different in HDPE than in PHBV. The nanotubes acts as a nucleating agent in HDPE matrix, increasing the melting temperature and enthalpy during melting (ΔH_m) as function as MWCNT amount. As a consequence, the degree of crystallinity of HDPE increase. No effect is observed in the melting temperature of PHBV, but its melting enthalpy and crystallinity was significantly reduced as MWCNT increases in the composite. This may be related to the fact that both polymers crystallize in the same temperature range, but the MWCNTs only act as nucleating agent in the HDPE matrix, hindering, probably, some of PHBV crystallization.

Table 2
Thermal properties for the pure polymers, blend and composites (average values and standard deviations in parentheses).

Sample	T_{m1} (°C)	T_{m2} (°C)	T_{c1} (°C)	T_{c2} (°C)	ΔH_{m1} (Xc_{HDPE})* (J/g_{HDPE})	ΔH_{m2} (Xc_{HDPE})* (J/g_{PHBV})	$T_{deg\ PE}$ (°C)	$T_{deg\ PHBV}$ (°C)
HDPE	132.6	-	108.4	-	176.4 (60.1)	-	482	-
PHBV	-	175.5	-	121.9	-	86.8 (59.2)	-	289
PE/PHBV	130.3	164.2	98.9	115.8	175.8 (59.9)	82.2 (56.1)	461	284
M1	135.6	164.7	98.8	116.5	204.2 (69.6)	64.0 (43.7)	475	279
M2	134.9	164.9	97.3	115.9	182.3 (62.1)	64.8 (44.2)	478	279
M3	133.8	165.0	96.0	115.5	175.2 (59.7)	69.1 (47.1)	475	284
M1*	140.2	163.3	80.6	116.3	155.9 (53.1)	33.5 (22.9)	477	287
M2*	136.9	161.9	75.5	117.7	190.9 (65.0)	48.0 (32.7)	478	281

*the crystallinity degree of each polymer (Xc), in percentage, is indicated in brackets.

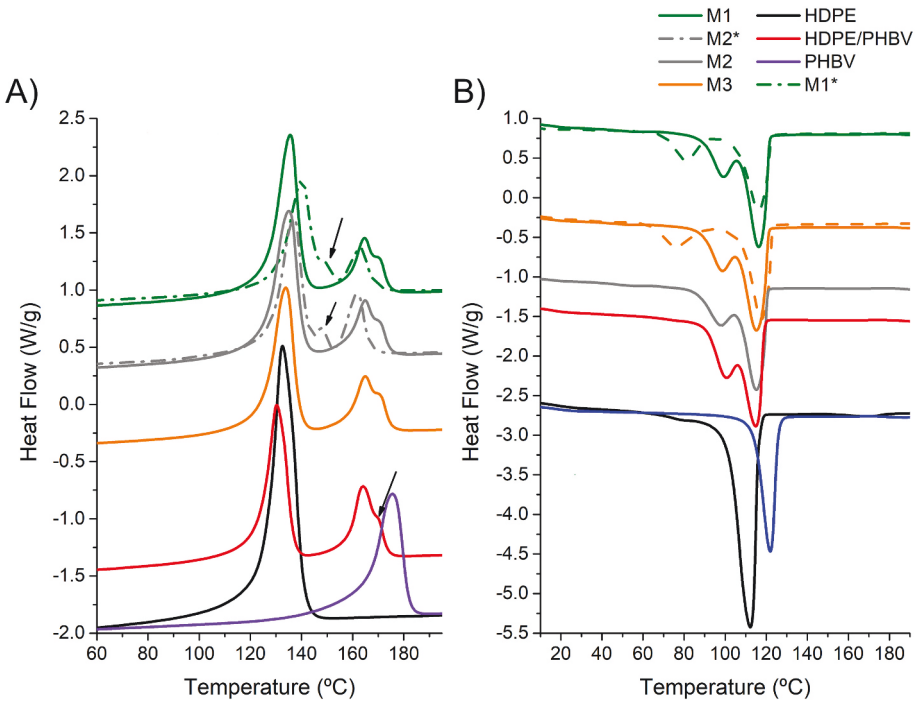

Fig. 4. DSC thermograms for PE, PHBV and composites; a) heating second scan, b) cooling scan.

In fact, it is important to note that MWCNTs are mainly dispersed in polyethylene matrix, as can be seen in morphological results.

When polyethylene grafted maleic anhydride is incorporated, the compatibility between the two polymers increases, leading to changes in their thermal properties.

The thermograms show an increase in the melting temperature of HDPE. The melting temperature of the PHBV decreases slightly, but the most remarkable issue is that the shoulder disappears at 170 °C. On the other hand, the thermograms show a third peak between the two (around 150 °C) (see Fig. 4a), probably related with the melting of imperfect crystals, which crystallized at low temperatures during the cooling scan and may have also experienced melting-recrystallization during the second DSC heating.

Thermogravimetric analysis (TGA) was used to evaluate the thermal degradation of the masterbach of PE (PE+15%MWCNTs), PHBV and composites. From Fig. 5 and Table 2 it is possible to state that PE masterbach degrades at 480 °C (above to PE pristine at 462 °C for the CNTs presence, not showed here) while PHBV have a degradation temperature around 280 °C. The TGA thermograms of HDPE/PHBV blend and MWCNT composites show two steps, a first one corresponding to the degradation temperature of PHBV (around 280 °C) and a second one, at a higher temperature, to HDPE. The incorporation of MWCNTs increases

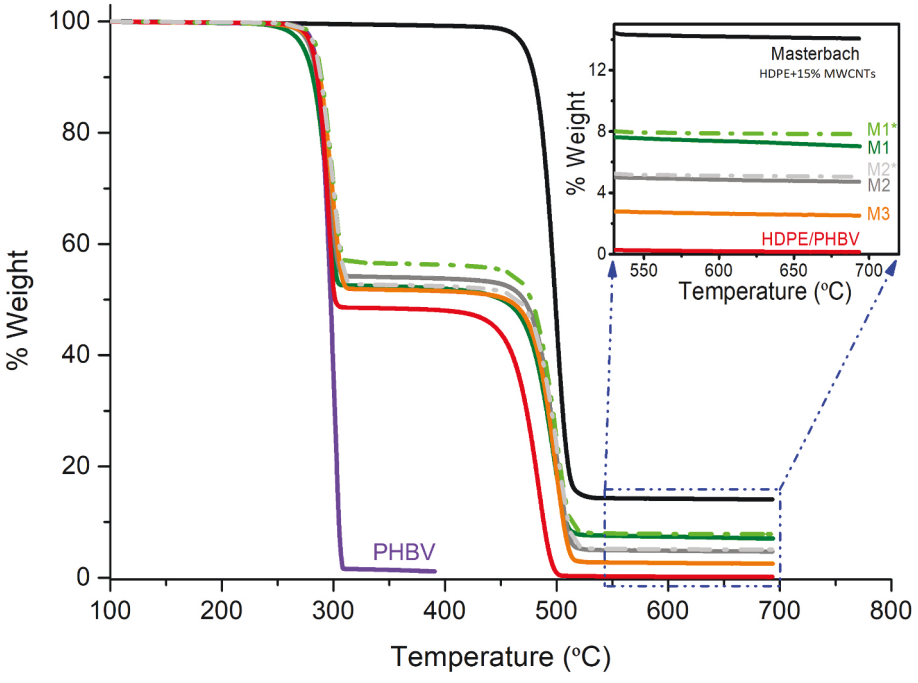

Fig. 5. TGA results for PE, PHBV and composites.

the thermal stability of the polyethylene part, while the degradation temperature of PHBV part decreases slightly with respect to the Tdeg in the HDPE/PHBV blend. This may be related to the fact that the nanotubes are more thermally stable and confined in the polyethylene matrix. In the nanocomposites thermograms, the residual mass, measured at 700 °C, agrees with the amount of MWCNTs incorporated in the matrix, which shows that the samples are homogeneous and that the actual amount of filler matches the nominal one.

3.4 *Mechanical properties*.

The modulus, strain and tensile strength at yield point and the same parameters and strain at break are presented in Table 3. While the HDPE shows a ductile behaviour, PHBV, HDPE/PHBV blend and composites are brittle materials, with a break point closer to the elastic limit. The stiffness of the blend shows an intermediate behaviour between the two immiscible polymers (as would be expected due to the lack of compatibility). Nevertheless, this drawback in mechanical properties must be assumed for obtaining a segregated network structure. When MWCNT are incorporated to the blend an enhancement in the modulus regarding to the blend is observed due to the higher rigidity of the filler. This is in agreement with the G' values obtained from the rheological properties. However, not important changes are observed in strain or tensile strength at break point indicating that are not produced changes in the ductility of the samples with MWCNT addition.

The principal aim of anhydride maleic incorporation into HDPE/PHBV/MWCNTs composite formulations was to achieve increased toughness and improved morphological (more uniform morphology) and rheological properties of the materials. The target was partially obtained because of the ductility improvement was scarce, respect the nanocomposites without MAPE, although was obtained in the case of morphological and rheological properties.

Hardness of pure polymers, blends and composites is presented in Table 3. Hardness of polymer blend is in the middle of HDPE and PHBV hardness, being higher in the case of PHBV as it is expected in a more fragile material. A hardness increase with nanotube amount it is observed that it is related with an expected increase of material rigidity with filler. With grafted PE an increase in hardness is observed that can be related with the increase in polymers compatibility and a better dispersion of nanotubes in the HDPE/PHBV matrix.

3.4. Electrical conductivity

Fig. 6 represents the electrical conductivity values of different composites. The addition of MWCNT increases the electrical conductivity of HDPE/PHBV blend (clearly electrical insulator) as a function of MWCNT amount up to a value of 5.29×10^{-2} S cm^{-1} measured in M1 with 7.5 wt% MWCNT. The degree of compatibilization achieved after the incorporation of polyethylene grafted with maleic anhydride in composites M1 and M2, allowed a significant increase in conductivity (near one order of magnitude in M1* and two orders of magnitude in M2* as presented in Table 2).

To obtain a conductive plastic that can be used to manufacture an electromagnetic shielding (EMI) chassis, the volume resistivity of the material must be 10^4 Ω cm or lower (same order of magnitude for surface resistivity). Since the electrical volume resistivity is inversely proportional to the electrical conductivity, the minimum conductivity value that guarantees that a certain EMI corresponds to a value of 10^{-4} S cm^{-1}. From the values displayed in Fig. 6, it can be concluded that M2 and M1 (with and without MAPE) composites are within the EMI shielding range, so the new formulations would be suitable for applications in this field.

Anyway, it must be taken into account that it is established that in order to achieve 99.9% attenuation of EMI radiation, which is considered an adequate level of protection for many applications, a shielding or shielding efficiency greater than 20 dB is needed. According to the bibliography, this target requires, theoretically, an electrical conductivity of 10^{-2} S cm^{-1} [6,7,17,18,42]. Taking into account values in Table 2 it can be observed that for composites M1, M1* and M2* a value of 99.9% attenuation is obtained.

With a 0.5% content of maleic anhydride, the electrical conductivity experiments an increase of two orders of magnitude in M2* composite with respect to M2 composite, and an increase of one order of magnitude in M1* with respect to M1. Therefore, the fact of introducing polyethylene grafted with maleic anhydride represents an appropriate strategy to enhance the electrical conductivity values. With the incorporation of maleic anhydride appropriate shielding values are obtained with a minor amount of MWCNTs. In fact, the conductivity value of M2 composite (5% MWCNT) is similar to the M1 value (7.5% MWCNT) without MAPE.

To confirm this results and to ensure that this values are suitable EMI applications theoretical shielding values were calculated as explained in experimental part. Fig. 7 shows the EMI shielding data for nanocomposites in the frequency range between 10^5 and 10^6 Hz. All composites display a shielding level constant over the studied frequency range. Again, the material with a better shielding behaviour is the M1*, with values around 80 dB but all of them are over the 20 dB value needed to obtain a 99.9% attenuation of EMI radiation adequate for use in electronic housings. The maleic anhydride addition improve shielding values related with the enhancemente in conductivity getting appropriate shielding values with a minor amount of filler (M2*).

In summary, it is worth noting that the nanocomposites which were partially compatible with MAPE, display a clearly higher ductility and hardness than the HDPE/PHBV blend, as well as electrical properties, as was the original goal.

Table 3
Mechanical properties for the pure polymers, blend and composites (average values and standard deviations in parentheses).

Sample	*E* (MPa)	σ_y (MPa)	ε_Y (%)	σ_B (MPa)	ε_B (%)	Hardness (Shore D)
PE	443 (42)	22.6 (0.4)	19.8 (0.6)	16.5 (2.0)	927.6 (71.7)	59.1 (0.4)
PHBV	1634 (141)	31.9 (1.9)	2.5 (0.1)	33.3 (4.7)	2.7 (0.4)	79.4 (0.8)
PE/ PHBV	775 (53)	19.6 (3.5)	3.5 (0.8)	18.7 (3.5)	3.8 (0.8)	64.5 (0.6)
M1	1247 (31)	27.0 (2.5)	3.4 (0.9)	26.7 (2.6)	3.5 (0.9)	68.1 (0.7)
M2	1156 (54)	22.6 (3.7)	4.0 (0.4)	22.4 (3.7)	4.2 (0.4)	66.8 (1.3)
M3	878 (61)	21.1 (3.4)	4.4 (0.6)	20.5 (3.2)	4.8 (0.7)	65.4 (0.7)
M1*	1201 (99)	24.4 (3.6)	3.6 (0.3)	24.2 (2.9)	4.2 (0.4)	71.4 (0.4)
M2*	1136 (88)	29.0 (1.2)	4.0 (0.3)	26.6 (4.2)	4.2 (0.4)	70.2 (0.4)

4. Conclusions

Polymer nanocomposites with electromagnetic shielding properties have been designed based on two polymeric immiscible matrices, HDPE and PHBV, in a 50/50 ratio by adding different amounts of MWCNTs (3.5 and 7.5%) and their physical properties characterized. The morphological images show composites with a typical morphology in an immiscible polymeric blend, confirmed by a double peak in DSC thermogram, where the MWCNTs are placed in HDPE matrix. This promotes an increase in the viscosity, with respect to pure polymers and polymer blend, and a plateau in moduli that indicates the formation of a percolated structure. In this structure the MWCNTs act as nucleants promoting an increase in thermal stability of PE. All nanocomposites show a certain level of conductivity but only composite with 7.5% of MWCNTs shows a conductivity value suitable for reaching 20 dB of electromagnetic shielding which is an adequate value for many applications.

When 0.5% of PE grafted with maleic anhydride was added to the compounds with 5% and 7.5% of nanotubes, the interfacial adhesion

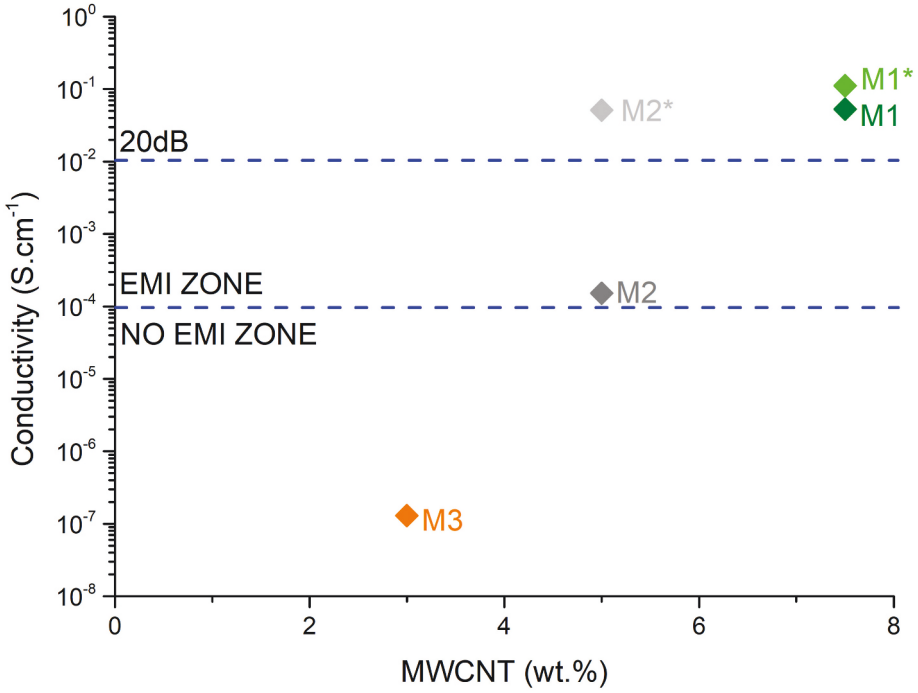

Fig. 6. Electrical conductivity result versus MWCNTs proportion in composites (Horizontal lines delimitates EMI ZONE, NO EMI ZONE and the 20 dB line from that an attenuation of 99,9% of EMI radiation is obtained).

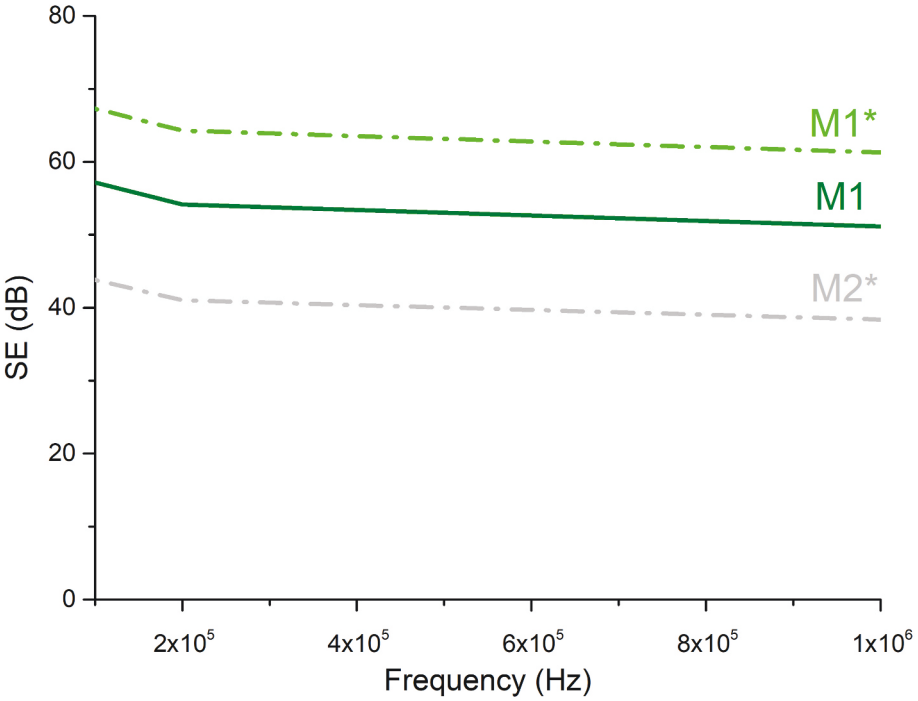

Fig. 7. The shielding effectiveness predictions according to Colanery and Shacklette [46].

between phases and the MWCNT dispersion improved causing an increase in conductivity that leads to a suitable EMI shielding level with a minor proportion of nanotubes. Nevertheless, no important effects are observed in mechanical properties.

Summarizing, the compounds with 5% and 7.5% of nanotubes and 0,5% of PE grafted are advanced sustainable composite materials, with adequate conductivity and electromagnetic shielding values for developing EMI shielding applications. This also constitutes a breakthrough for industrial applications where environmentally friendly polymers are increasingly required with identical performance as conventional polymers.

Author statement

David Fernández Armada: Investigation, Writing - Original Draft. Victoria González Rodríguez: Conceptualization, Validation, Writing -

Review & Editing. Pedro Costa: Methodology, Investigation. Senentxu Lanceros-Mendez: Writing - Review & Editing. Goretti Arias-Ferreiro: Investigation, Visualization. María-José Abad: Writing - Review & Editing, Funding acquisition. Ana Ares-Pernas: Conceptualization, Methodology, Writing - Review & Editing, Supervision.

Declaration of competing interest

The authors declare that they have no known competing financial interests or personal relationships that could have appeared to influence the work reported in this paper.

Acknowledgments

The authors would like to thank the financial support from Ministerio de Ciencia e Innovacion/FEDER (project ref; PID2020-116976RB-I00) and Xunta de Galicia-FEDER (Program of Consolidation and structuring competitive research units (ED431C 2019/17).

Furthermore, the authors thank the financial funding received from the Xunta de Galicia and the European Union (Program to support the predoctoral stage at SUG 2019 (ED481A-2019/001)).

Finally, the authors thank the Fundação para a Ciência e Tecnologia (FCT) for financial support in the framework of the Strategic Programs UID/FIS/04650/2020 and the grant SFRH/BPD/110914/2015 (PC), as well as to the Basque Government Industry Departments for support under the ELKARTEK program.

References

[1] S. Mondal, L. Nayak, M. Rahaman, A. Aldalbahi, T.K. Chaki, D. Khastgir, N.C. Das, An effective strategy to enhance mechanical, electrical, and electromagnetic shielding effectiveness of chlorinated polyethylene-carbon nanofiber nanocomposites, Compos. B Eng. 109 (2017) 155–169, https://doi.org/10.1016/j.compositesb.2016.10.049.

[2] V.P. Anju, M. Manoj, P. Mohanan, S.K. Narayanankutty, A comparative study on electromagnetic interference shielding effectiveness of carbon nanofiber and nanofibrillated cellulose composites, Synth. Met. 247 (2019) 285–297, https://doi.org/10.1016/j.synthmet.2018.12.021.

[3] P. Verma, P. Saini, R.S. Malik, V. Choudhary, Excellent electromagnetic interference shielding and mechanical properties of high loading carbon-nanotubes/polymer composites designed using melt recirculation equipped twin-screw extruder, Carbon N. Y. 89 (2015) 308–317, https://doi.org/10.1016/j.carbon.2015.03.063.

[4] D.W. Lee, J. Park, B.J. Kim, H. Kim, C. Choi, R.H. Baughman, S.J. Kim, Y.T. Kim, Enhancement of electromagnetic interference shielding effectiveness with alignment of spinnable multiwalled carbon nanotubes, Carbon N. Y. 142 (2019) 528–534, https://doi.org/10.1016/j.carbon.2018.10.076.

[5] M.H. Al-Saleh, W.H. Saadeh, U. Sundararaj, EMI shielding effectiveness of carbon based nanostructured polymeric materials: a comparative study, Carbon N. Y. 60 (2013) 146–156, https://doi.org/10.1016/j.carbon.2013.04.008.

[6] L. Vovchenko, L. Matzui, V. Oliynyk, V. Launets, Y. Mamunya, O. Maruzhenko, Nanocarbon/polyethylene composites with segregated conductive network for electromagnetic interference shielding, Mol. Cryst. Liq. Cryst. 672 (2018) 186–198, https://doi.org/10.1080/15421406.2018.1555349.

[7] H.Y. Wu, Y.P. Zhang, L.C. Jia, D.X. Yan, J.F. Gao, Z.M. Li, Injection molded segregated carbon nanotube/polypropylene composite for efficient electromagnetic interference shielding, Ind. Eng. Chem. Res. 57 (2018) 12378–12385, https://doi.org/10.1021/acs.iecr.8b02293.

[8] S. Kim, J.S. Oh, M.G. Kim, W. Jang, M. Wang, Y. Kim, H.W. Seo, Y.C. Kim, J.H. Lee, Y. Lee, J. Do Nam, Electromagnetic interference (EMI) transparent shielding of reduced graphene oxide (RGO) interleaved structure fabricated by electrophoretic deposition, ACS Appl. Mater. Interfaces 6 (2014) 17647–17653, https://doi.org/10.1021/am503893v.

[9] J. Joseph, A. Sharma, B. Sahoo, J. Paul, A.M. Sidpara, PVA/MLG/MWCNT hybrid composites for X band EMI shielding – study of mechanical, electrical, thermal and tribological properties, Mater, Today Commun 23 (2020), 100941, https://doi.org/10.1016/j.mtcomm.2020.100941.

[10] N.C. Das, T.K. Chaki, D. Khastgir, A. Chakraborty, Electromagnetic interference shielding effectiveness of conductive carbon black and carbon fiber-filled composites based on rubber and rubber blends, Adv. Polym. Technol. 20 (2000) 226–236, https://doi.org/10.1002/adv.1018.

[11] M. Rahaman, T.K. Chaki, D. Khastgir, Development of high performance EMI shielding material from EVA, NBR, and their blends: effect of carbon black structure, J. Mater. Sci. 46 (2011) 3989–3999, https://doi.org/10.1007/s10853-011-5326-x.

[12] Y. Kato, M. Horibe, S. Ata, T. Yamada, K. Hata, Stretchable electromagnetic-interference shielding materials made of a long single-walled carbon-nanotube-elastomer composite, RSC Adv. 7 (2017) 10841–10847, https://doi.org/10.1039/c6ra25350d.

[13] Z. Liu, G. Bai, Y. Huang, Y. Ma, F. Du, F. Li, T. Guo, Y. Chen, Reflection and absorption contributions to the electromagnetic interference shielding of single-walled carbon nanotube/polyurethane composites, Carbon N. Y. 45 (2007) 821–827, https://doi.org/10.1016/j.carbon.2006.11.020.

[14] S. Mondal, P. Das, S. Ganguly, R. Ravindren, S. Remanan, P. Bhawal, T.K. Das, N. C. Das, Thermal-air ageing treatment on mechanical, electrical, and electromagnetic interference shielding properties of lightweight carbon nanotube based polymer nanocomposites, Compos. Part A Appl. Sci. Manuf. 107 (2018) 447–460, https://doi.org/10.1016/j.compositesa.2018.01.025.

[15] Z. Zeng, M. Chen, H. Jin, W. Li, X. Xue, L. Zhou, Y. Pei, H. Zhang, Z. Zhang, Thin and flexible multi-walled carbon nanotube/waterborne polyurethane composites with high-performance electromagnetic interference shielding, Carbon N. Y. 96 (2016) 768–777, https://doi.org/10.1016/j.carbon.2015.10.004.

[16] N. Chikyu, T. Nakano, G. Kletetschka, Y. Inoue, Excellent electromagnetic interference shielding characteristics of a unidirectionally oriented thin multiwalled carbon nanotube/polyethylene film, Mater. Des. 195 (2020), 108918, https://doi.org/10.1016/j.matdes.2020.108918.

[17] L.C. Jia, D.X. Yan, C.H. Cui, X. Jiang, X. Ji, Z.M. Li, Electrically conductive and electromagnetic interference shielding of polyethylene composites with devisable carbon nanotube networks, J. Mater. Chem. C. 3 (2015) 9369–9378, https://doi.org/10.1039/c5tc01822f.

[18] M.H. Al-Saleh, Electrical, EMI shielding and tensile properties of PP/PE blends filled with GNP:CNT hybrid nanofiller, Synth. Met. 217 (2016) 322–330, https://doi.org/10.1016/j.synthmet.2016.04.023.

[19] S.G. Pardo, L. Arboleda, A. Ares, X. García, S. Dopico, M.J. Abad, Toughening strategies of carbon nanotube/polycarbonate composites with electromagnetic interference shielding properties, Polym. Compos. 34 (2013) 1938–1949, https://doi.org/10.1002/pc.22601.

[20] H. Pang, L. Xu, D.X. Yan, Z.M. Li, Conductive polymer composites with segregated structures, Prog. Polym. Sci. 39 (2014) 1908–1933, https://doi.org/10.1016/j.progpolymsci.2014.07.007.

[21] L. Arboleda-Clemente, A. Ares-Pernas, X. García, S. Dopico, M.J. Abad, Segregated conductive network of MWCNT in PA12/PA6 composites: electrical and rheological behavior, Polym. Compos. 38 (2017) 2679–2686, https://doi.org/10.1002/pc.23865.

[22] A.M. Kunjappan, A. Reghunadhan, A.A. Ramachandran, L. Mathew, M. Padmanabhan, D. Laroze, S. Thomas, Thin and efficient EMI shielding materials from binary thermoplastic blend nanocomposites, Polym. Adv. Technol. 33 (2022) 966–979, https://doi.org/10.1002/pat.5571.

[23] C. Lencar, S. Ramakrishnan, E. Erfanian, U. Sundararaj, The role of phase migration of carbon nanotubes in melt-mixed PVDF/PE polymer blends for high conductivity and EMI shielding applications, Molecules 27 (2022) 933.

[24] X. Zhang, C. Fan, Y. Ma, H. Zhao, J. Sui, J. Liu, C. Sun, Elastic composites fabricating for electromagnetic interference shielding based on MWCNTs and Fe3O4 unique distribution in immiscible NR/NBR blends, Polym. Eng. Sci. (2022) 1–12, https://doi.org/10.1002/pen.25985.

[25] H. Zhang, Z. Heng, J. Zhou, Y. Shi, Y. Chen, H. Zou, M. Liang, In-situ co-continuous conductive network induced by carbon nanotubes in epoxy composites with enhanced electromagnetic interference shielding performance, Chem. Eng. J. 398 (2020), 125559, https://doi.org/10.1016/j.cej.2020.125559.

[26] S.M.N. Sultana, S.P. Pawar, M. Kamkar, U. Sundararaj, Tailoring MWCNT dispersion, blend morphology and EMI shielding properties by sequential mixing strategy in immiscible PS/PVDF blends, J. Electron. Mater. 49 (2020) 1588–1600, https://doi.org/10.1007/s11664-019-07371-8.

[27] M. Wang, X.H. Tang, J.H. Cai, H. Wu, J. Bin Shen, S.Y. Guo, Construction, mechanism and prospective of conductive polymer composites with multiple interfaces for electromagnetic interference shielding: a review, Carbon N. Y. 177 (2021) 377–402, https://doi.org/10.1016/j.carbon.2021.02.047.

[28] Y.F. Liu, L.M. Feng, Y.F. Chen, Y.D. Shi, X.D. Chen, M. Wang, Segregated polypropylene/cross-linked poly(ethylene-co-1-octene)/multi-walled carbon nanotube nanocomposites with low percolation threshold and dominated negative temperature coefficient effect: towards electromagnetic interference shielding and thermistors, Compos. Sci. Technol. 159 (2018) 152–161, https://doi.org/10.1016/j.compscitech.2018.02.041.

[29] T.N. Yue, Y.N. Gao, Y. Wang, Y.D. Shi, J. bin Shen, H. Wu, M. Wang, Processing temperature-dependent distribution of multiwall carbon nanotube in poly (ethylene-co-1-octene)/high density polyethylene for electrical conductivity and microwave shielding enhancement, Polym. Compos. 42 (2021) 1396–1406, https://doi.org/10.1002/pc.25910.

[30] L.S. Montagna, I.C. Oyama, R.C.B.C. Lamparelli, A.P. Silva, T.L.A. Montanheiro, A. P. Lemes, Evaluation of biodegradation in aqueous medium of poly (Hydroxybutyrate-Co-hydroxyvalerate)/carbon nanotubes films in respirometric system, J. Renew. Mater. 7 (2019) 117–128, https://doi.org/10.32604/jrm.2019.00036.

[31] C.M. Chan, S. Pratt, P. Halley, D. Richardson, A. Werker, B. Laycock, L.J. Vandi, Mechanical and physical stability of polyhydroxyalkanoate (PHA)-based wood plastic composites (WPCs) under natural weathering, Polym. Test. 73 (2019) 214–221, https://doi.org/10.1016/j.polymertesting.2018.11.028.

[32] H. Ebrahimi, F. Sharif, S.A.A. Ramazani, in: J. Polym, English (Eds.), Effects of Modified Titanium Dioxide Nanoparticles on the Thermal and Mechanical Properties of Poly(l-Lactide)-B-Poly(ε-Caprolactone), 2022, https://doi.org/10.1007/s13726-022-01039-7. Iran.

[33] Y. Liu, H. He, G. Tian, Y. Wang, J. Gao, C. Wang, L. Xu, H. Zhang, Morphology evolution to form double percolation polylactide/polycaprolactone/MWCNTs

nanocomposites with ultralow percolation threshold and excellent EMI shielding, Compos. Sci. Technol. 214 (2021), https://doi.org/10.1016/j.compscitech.2021.108956.
[34] C.M. Chan, L.J. Vandi, S. Pratt, P. Halley, D. Richardson, A. Werker, B. Laycock, Insights into the biodegradation of PHA/wood composites: micro- and macroscopic changes, Sustain. Mater. Technol. 21 (2019), e00099, https://doi.org/10.1016/j.susmat.2019.e00099.
[35] B. Rani-Borges, A.U. Faria, A. De Campos, S.P.C. Gonçalves, S.M. Martins-Franchetti, Biodegradation of additive PHBV/PP-co-PE films buried in soil, Polimeros 26 (2016) 161–167, https://doi.org/10.1590/0104-1428.2127.
[36] M.N.F. Norrrahim, H. Ariffin, M.A. Hassan, N.A. Ibrahim, H. Nishida, Performance evaluation and chemical recyclability of a polyethylene/poly(3- hydroxybutyrate-co-3-hydroxyvalerate) blend for sustainable packaging, RSC Adv. 3 (2013) 24378–24388, https://doi.org/10.1039/c3ra43632b.
[37] T.M. Passos, J.C. Marconato, M.S. Ranchetti Martins, Biodegradation of films of low density polyethylene (LDPE), (70/30) blend with Paecilomyces variotii, Polímeros. 25 (2015) 29–34, https://doi.org/10.1590/0104-1428.1432.
[38] S.P.C. Gonçalves, S.M.M. Franchetti, Biodegradation of PP and PE blended with PHBV in soil samples, Adv. Polym. Technol. 34 (2014) 1–8, https://doi.org/10.1002/adv.21486.
[39] A.P. da Silva, T.L. do Amaral Montanheiro, L. Stieven Montagna, P.F. Andrade, N. Durán, A.P. Lemes, Effect of carbon nanotubes on the biodegradability of poly (3-hydroxybutyrate-co-3-hydroxyvalerate) nanocomposites, J. Appl. Polym. Sci. 136 (2019) 1–10, https://doi.org/10.1002/app.48020.
[40] R.A. Qazi, M.S. Khan, L.A. Shah, R. Ullah, A. Kausar, R. Khattak, Eco-friendly electronics, based on nanocomposites of biopolyester reinforced with carbon nanotubes: a review, Polym. Technol. Mater. 59 (2020) 928–951, https://doi.org/10.1080/25740881.2020.1719137.
[41] G.F. Shan, X. Gong, W.P. Chen, L. Chen, M.F. Zhu, Effect of multi-walled carbon nanotubes on crystallization behavior of poly(3-hydroxybutyrate-co-3-hydroxyvalerate), Colloid Polym. Sci. 289 (2011) 1005–1014, https://doi.org/10.1007/s00396-011-2412-1.
[42] S.H. Lee, Y. Lee, M.G. Jang, C. Han, W.N. Kim, Comparative study of EMI shielding effectiveness for carbon fiber pultruded polypropylene/poly(lactic acid)/multiwall CNT composites prepared by injection molding versus screw extrusion, J. Appl. Polym. Sci. 134 (2017) 1–11, https://doi.org/10.1002/app.45222.
[43] B.G. Soares, E. Cordeiro, J. Maia, E.C.L. Pereira, A.A. Silva, The effect of the noncovalent functionalization of CNT by ionic liquid on electrical conductivity and electromagnetic interference shielding effectiveness of semi-biodegradable polypropylene/poly(lactic acid) composites, Polym. Compos. 41 (2020) 82–93, https://doi.org/10.1002/pc.25347.
[44] Y.J. Tan, J. Li, X.H. Tang, T.N. Yue, M. Wang, Effect of phase morphology and distribution of multi-walled carbon nanotubes on microwave shielding of poly(L-lactide)/poly(ε-caprolactone) composites, Compos. Part A Appl. Sci. Manuf. 137 (2020), 106008, https://doi.org/10.1016/j.compositesa.2020.106008.
[45] B. Wunderlich, Chapter 2 - the basis OF thermal analysis, in: B. Wunderlich (Ed.), Therm. Anal., Academic Press, 1990, pp. 37–78, https://doi.org/10.1016/B978-0-12-765605-2.50006-6.
[46] N.F. Colaneri, L.W. Shacklette, EMI shielding measurements of conductive polymer blends, IEEE Trans. Instrum. Meas. 41 (1992) 291–297, https://doi.org/10.1109/19.137363.
[47] S. Yang, K. Lozano, A. Lomeli, H.D. Foltz, R. Jones, Electromagnetic interference shielding effectiveness of carbon nanofiber/LCP composites, Compos. Part A Appl. Sci. Manuf. 36 (2005) 691–697, https://doi.org/10.1016/j.compositesa.2004.07.009.
[48] P. Pötschke, T.D. Fornes, D.R. Paul, Rheological behavior of multiwalled carbon nanotube/polycarbonate composites, Polymer 43 (2002) 3247–3255, https://doi.org/10.1016/S0032-3861(02)00151-9.
[49] A. Ares, S.G. Pardo, M.J. Abad, J. Cano, L. Barral, Effect of aminomethoxy silane and olefin block copolymer on rheomechanical and morphological behavior of fly ash-filled polypropylene composites, Rheol. Acta 49 (2010) 607–618, https://doi.org/10.1007/s00397-009-0417-1.
[50] S.A.R. Hashmi, U.K. Dwivedi, N. Chand, Graphite modified cotton fibre reinforced polyester composites under sliding wear conditions, Wear 262 (2007) 1426–1432, https://doi.org/10.1016/j.wear.2007.01.014.
[51] O. Bera, M. Trunec, Oscillatory shear rheology of polystyrene melts filled with carbon black and fullerene, Plast. Rubber Compos. 41 (2012) 384–389, https://doi.org/10.1179/1743289812Y.0000000008.
[52] A. Paleo, V. Sencadas, F.W. van Hattum, S. Lanceros-Méndez, A. Ares, Carbon nanofiber type and content dependence of thePhysical properties of carbon nanofiber ReinforcedPolypropylene composites, Polym. Eng. Sci. 54 (2014) 117–12812, https://doi.org/10.1002/pen.23539.
[53] A. Ares, A. Lasagabaster, M.J. Abad, R. Noguerol, C. Cerecedo, V. Valcárcel, J. M. Caamaño, F. Guitián, Effects of silane functionalization of alumina whiskers on high-density polyethylene composites, J. Compos. Mater. 48 (2014) 3141–3151, https://doi.org/10.1177/0021998313507615.
[54] L. Arboleda-Clemente, A. Ares-Pernas, X.X. García-Fonte, M.J. Abad, Water sorption of PA12/PA6/MWCNT composites with a segregated conductive network: structure–property relationships, J. Mater. Sci. 51 (2016) 8674–8686, https://doi.org/10.1007/s10853-016-0127-x.
[55] L. Arboleda-Clemente, A. Ares-Pernas, X. García, S. Dopico, M.J. Abad, Influence of polyamide ratio on the CNT dispersion in polyamide 66/6 blends by dilution of PA66 or PA6-MWCNT masterbatches, Synth. Met. 221 (2016) 134–141, https://doi.org/10.1016/J.SYNTHMET.2016.07.030.
[56] X. García-Fonte, A. Ares-Pernas, C. Cerecedo, V. Valcárcel, M.J. Abad, Influence of phase morphology on the rheology and thermal conductivity of HDPE/PA6 immiscible blends with alumina whiskers, Polym. Test. 71 (2018) 56–64, https://doi.org/10.1016/J.POLYMERTESTING.2018.08.012.